Korean Chem. Eng. Res., 53(5), 565-569 (2015)
http://dx.doi.org/10.9713/kcer.2015.53.5.565
PISSN 0304-128X, EISSN 2233-9558

CoO Thin Nanosheets Exhibit Higher Antimicrobial Activity Against Tested Gram-positive Bacteria Than Gram-negative Bacteria

Shams Tabrez Khan*,†, Rizwan Wahab*,†, Javed Ahmad*, Abdulaziz A. Al-Khedhairy*, Maqsood A. Siddiqui*, Quaiser Saquib*, Bahy A. Ali*, and Javed Musarrat*****

*Department Zoology, King Saud University, Riyadh 11451, Saudi Arabia
**Department of Nucleic Acids Research, Genetic Engineering and Biotechnology Research Institute, City for Scientific Research and Technological Applications, Alexandria, Egypt
***Department of Agricultural Microbiology, Faculty of Agricultural Sciences, Aligarh Muslim University, Aligarh 202002, India.
(Received 16 November 2014; Received in revised form 27 January 2015; accepted 27 January 2015)

Abstract – Envisaging the role of Co in theranautics and biomedicine it is immensely important to evaluate its antimicrobial activity. Hence in this study CoO thin nanosheets (CoO-TNs) were synthesized using wet chemical solution method at a very low refluxing temperature (90 °C) and short time (60 min). Scanning electron microscopy of the grown structure revealed microflowers (2~3 μm) composed of thin sheets petals (60~80 nm). The thickness of each individual grown sheet varies from 10~20 nm. Antimicrobial activities of CoO-TNs against two Gram positive bacteria (*Micrococcus luteus*, and *Staphylococcus aureus*), and two Gram negative bacteria (*Escherichia coli* and *Pseudomonas aeruginosa*) were determined. A 98% and 65% growth inhibition of *M. luteus* and *S. aureus* respectively, was observed with 500 μg/ml of CoO-TNs compared to 39 and 34% growth inhibition of *E. coli* and *P. aeruginosa*, respectively with the same concentration of CoO-TNs. Hence, synthesized CoO-TNs exhibited antimicrobial activity against Gram negative bacteria and an invariably higher activity against tested Gram positive bacteria. Therefore, synthesized CoO-TNs are less prone to microbial infections.

Key words: Nanostructures, CoO-TNs, Antibacterial Activity, Theranautics

1. Introduction

Metallic nanoparticles (NPs) with different structures and properties represent an enormous opportunity in medical field due to their small size and shape [1-3]. Therefore, many new NPs with interesting properties and potential applications in theranautics and biomedicine are being synthesized [4-6]. Among various nanocompounds, cobalt nanoparticles (CoNPs) are of special interest as they display a wealth of size-dependent catalytic, electronic, magnetic, and structural properties. Owing to these properties, CoO-NPs offer powerful tools for research activity and have been proposed for a number of applications in different fields including theranautics and biomedicine as reviewed by Akbarzadeh *et al.* [7]. Wang *et al*., [8] designed a novel glucose biosensor using nanoscaled cobalt phthalocyanine (NanoCoPc)-glucose oxidase (GOD) biocomposite. Recently Kainz *et al*., synthesized carbon coated cobalt nanoparticles for their potential use in biomedicine [9]. Co and CoPt are traditionally synthesized using carbonyl pyrolysis [10-12]. However, other methods such as solution phase metal salt reduction are also being used for the synthesis of CoO nanocrystals. CoO nanocrystals are being studied for hydrogenolysis [13], CO oxidation [14], and for their electrochemical behaviors [15]. Wang *et al*. reported the synthesized octahedral CoO nanocrystals of 200 nm or even larger and studied their electrochemical performance [16]. Zhang *et al*. has also reported synthesis of CoO nano crystals with various morphologies [17]. As it is difficult to obtain pure CoO, techniques like laser vaporization controlled condensation are being used for the synthesis of CoO nano particles [18].

The present work, reports new simple and mild procedure for the synthesis of pure CoO microflowers composed with thin sheets (CoO-TNs), using cobalt nitrate hexahydrate ($Co(NO_3)_2.6H_2O$) and sodium hydroxide (NaOH). Considering, the proposed use of cobalt-based NPs in biomedicine and theranautics, it is important to evaluate their antimicrobial activities as many biomaterials are prone to microbial infections [19-20] posing a serious health risk. To the best of our knowledge, there is only one report on the antimicrobial activity of CoO nanostructures [21]. This study focuses on the modulation of synthetic parameters and arrangement of cobalt microflowers composed with thin nanosheets and their antimicrobial activity.

2. Experimental

2-1. Material and methods

2-1-1. Synthesis of cobalt oxide micro-flowers composed with thin nanosheets (CoO-TNs)

CoO-TNs were synthesized using cobalt nitrate hexahydrate ($Co(NO_3)_2$.

† To whom correspondence should be addressed.
E-mail: rwahab@ksu.edu.sa, shamsalig75@gmail.com

$6H_2O$) and sodium hydroxide (NaOH) purchased from Aldrich chemical Co., USA and used without further purification. In a typical experiment: The $Co(NO_3)_2.6H_2O$ (10 mM, 0.1455 g) and NaOH (0.1M, 0.2 g) were mixed in 50 ml of double deionized distilled water (DDDW) under constant stirring for 30 min. The pH of the solution was measured and controlled using ion analyser (corning P^H meter 430 red, coleparmer, U.S.A) till it reached up to 12.30. After the complete dissolution, solution was transferred in to a refluxing pot and refluxed at 90 °C for 1 h. As the refluxing temperature rises, the color of the solution changes from dark red to black. After refluxing, the precipitate was washed to remove ionic impurities with alcohol (methanol, ethanol) and acetone several times. The black powder sample was dried in a glass Petridish at room temperature and was finally collected in a clean glass sample vial for further analysis.

2-1-2. Characterization of synthesized CoO-TNs

The morphology of the black colored grown powder was observed via scanning electron microscopy (SEM, JSM-6380 LA, Japan). For SEM observation, powder was uniformly spread on a carbon tape and coated with thin conducting layer of platinum for 3 sec. The crystallinity and phases of black colored powder was characterized with X-ray powder diffractometer (XRD, PANalytical XPert Pro, U.S.A.) with $Cu_{K\alpha}$ radiation (λ=1.54178Å) in range from 20-80º with 6º/min scanning speed. The elemental composition was examined by using energy dispersive spectroscopy (EDS), attached with scanning electron microscopy at room temperature (Jeol, JED-2200 series, Japan).

2-1-3. Antimicrobial activity of CoO-TNs

Growth inhibition experiments were performed by determining the optical density at 600 nm of bacteria grown without or with various concentrations of CoO-TNs (25, 50, 100, 200, 300 and 500 μg/ml). Antibacterial activity against two strains each of Gram negative (*E. coli* and *P. aeruginosa*), and Gram positive bacteria (*S. aureus*, and *M. luteus*) was determined. Cells of *E. coli*, *P. aeruginosa*, *M. luteus* and *S. aureus* were grown to late log phase in autoclaved Luria broth (HiMedia), nutrient broth (HiMedia), Mueller-Hinton broth (HiMedia), and brain heart infusion broth (HiMedia) respectively. An aliquot of 500 μl from these cultures were added to fresh 5 ml sterile broths amended with various concentrations of CoO-TNs (25, 50, 100, 200, 300 and 500 μg/ml). Absorbance at a wave length of 600 nm (OD600) was determined after every 2 h using Elisa reader (Multiskan Ex, Thermo Scientific, Finland). Change in absorbance at 600 nm was calculated by subtracting the OD600 at 0 h from the OD600 at a given time. Results presented are the mean ± standard error of three independent experiments each. *p*-values were calculated using an unpaired Student's *t* test of GraphPad software (GraphPad Software, Inc., USA). *p*-values considered significant (p <0.05) are marked with asterisk in the figures. Percent growth inhibition was calculated by comparing the net change in OD600 obtained for control to those obtained for a treatment at a given time.

3. Result and Discussion

3-1. Morphological and crystalline property of synthesized CoO-TNs

The X-ray diffraction pattern (XRD) defines, the crystalline property of grown CoO-TNs powder and characterized at above parameters. Peaks at positions 33.54, 36.39, 37.39, 43.67, 50.84 and 65.09 denotes the diffractions of <220, <311, <222, <400, <331 and <440, matching well with the lattice constants of cobalt oxide a=b=c 8.084 Å (Fig. 1), as described by the Joint Committee on Powder Diffraction Standards (JCPDS 43-1003). In XRD spectrum no other peak was observed except CoO, which further confirms that grown product is pure CoO and is free from chemical impurities. Additionally, intensities of diffraction peaks in the spectrum confirms the formation of CoO-TNs.

3-1-1. Morphological analysis (SEM results)

A low magnification SEM image (Fig. 2a) of CoO-TNs, shows that the nanostructure was arranged with the assortment of several thin sheets. From the SEM image it appears that the structural particles are joined together to from a flowers shaped morphology composed with thin nanosheets (TNs). A further clarification of size and shape of the grown flowers shaped microstructures was confirmed with high magnification images (Fig. 2b). These images indicate that the estimated diameter of each individual flower shaped structure is in the range of 2-3 μm. It is also evident from the obtained image that the size of each sheet particle is in the range of 60-80 nm and thickness varies from 10-20 nm, surfaces are smooth and flat. The size of grown particles was clearly in agreement with X-ray diffraction analysis and analogous to SEM images (Fig. 2b) [18].

The elemental composition of grown microstructures composed with thin nanosheets (CoO-TNs) was observed via EDS spectroscopy equipped with SEM micrograph (Fig. 3). It is clearly seen from the EDS spectrum that cobalt and oxygen peaks appeared in the spectrum, which again reveals that the formed structures were made by cobalt and oxygen. No other impurity related to other element was

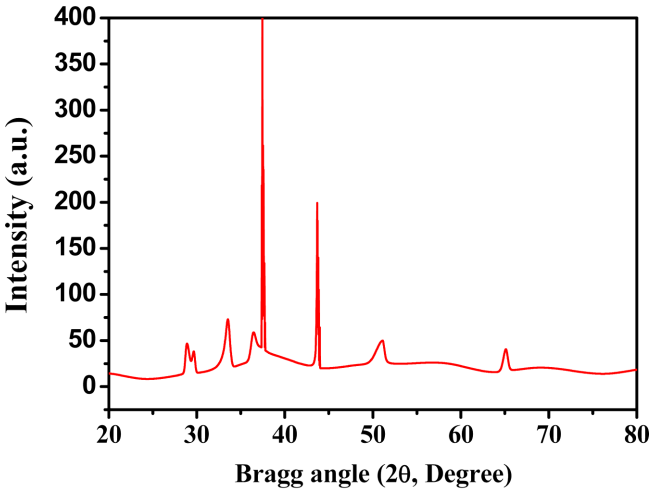

Fig. 1. X-ray diffraction pattern (XRD) of grown CoO-TNs.

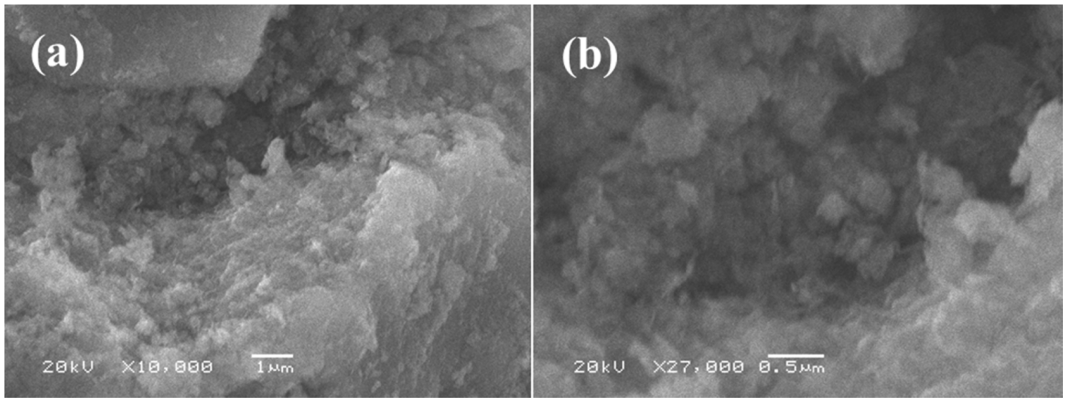

Fig. 2. Typical low (a) & high (b) magnified scanning electron microscopic (SEM) images of as-grown cobalt oxide microflowers composed with thin nanosheets refluxed at 90 °C for 1 h.

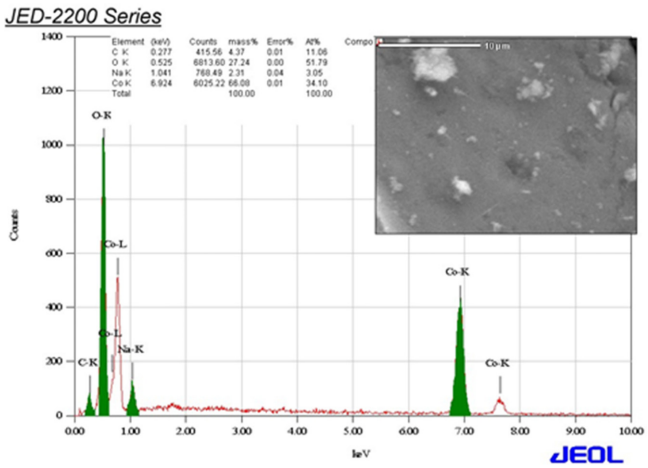

Fig. 3. Energy dispersive spectra (EDS) of synthesized CoO-TNs.

found in the spectrum further confirming that the synthesized structures are pure CoO.

3-1-2. Possible proposed mechanism for the formation of CoO-TNs nanostructure

On the basis of the experimental data (crystalline property, chemical analysis and morphological character), we have proposed a chemical reaction and schematic mechanism for the formation of CoO-TNs microstructures composed with thin nanosheets. As we know that the chemical precipitation synthesis of nano and microstructures is a technique by which, we can prepare various types of materials such as metal oxide, composite, and organic-inorganic etc, at a relatively low temperature. In our experiment, the aqueous solution of $Co(NO_3)_2.6H_2O$ was used, which appeared as dark red colored solution under constant stirring. To this aqueous suspension, when NaOH (0.2M) was added dropwise, the color of the solution changed ultimately to wine red. The pH of the solution was monitored till it reached to 12.30. The solution of $Co(NO_3)_2.6H_2O$ and NaOH was transferred to two necked refluxing pot and refluxed at 90 °C for 1 h in refluxing mental. As the reaction proceeds with increase of temperature, the dark red colored solution of cobalt changes to black within 10-15 min. During the precipitation process, NaOH played an important role in nucleation and growth of microflowers composed with thin nanosheets. In solution hydroxyl (OH^-) ions from sodium hydroxide reacts with nitrate chain of cobalt to form cobalt hydroxide ($Co(OH)_2$) and sodium nitrate ($NaNO_3$) (equation 1). As the temperature of refluxing pot increases and reaches to an optimum, hydroxide molecule of cobalt change to oxide form i.e. cobalt oxide (equation 2). Initially, in nucleation phase, the small dots were formed in the refluxing pot and as the temperature increases, these small dots changes to small cores in solution (Fig. 4a). As the refluxing temperature rises further, hydroxide molecule change to oxide molecules. In this experiment it is assumed that after acquiring sufficient thermal energy from the refluxing pot, the aggregated molecules arrange themselves to form small spherical core cells (Fig. 4b). The size of these core cells increases with temperature of refluxing pot. On the surface of core cells flower rachis was formed, which provides the attachment/growth of base plates/thinsheets of CoO microflowers (Fig. 4c). As the refluxing temperature increases the boundaries and side walls of thin sheets are arranged due to surface attachment of hydroxyl ions in solution. Due to the continuous deposition of hydroxyl ions on the surface of core shells more and more sheets are formed. When the molecules become saturated at their ideal refluxing temperature, structures fully grows and form flower like morphology

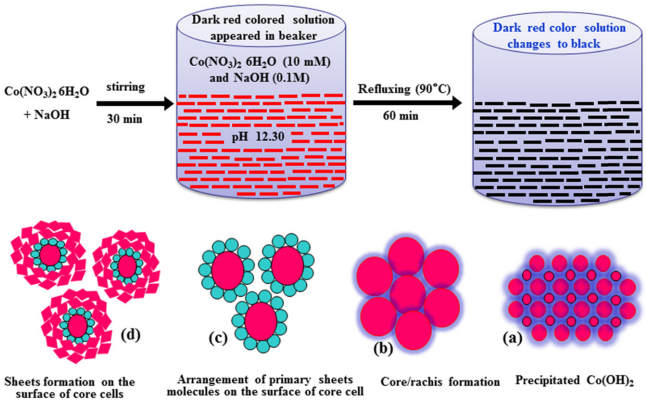

Fig. 4. Possible proposed mechanism for the formation of CoO-TNs.

(Fig. 4d). The simple chemical reaction is specified in the reaction steps (1) and (2) for the solution of copper nitrate hexa hydrate ($Co(NO_3)_2 \cdot 6H_2O$) and alkali sodium hydroxide (NaOH).

$$Co(NO_3)_2 \cdot 6H_2O + 2NaOH \longrightarrow Co(OH)_2 + 2NaNO_3 + 6H_2O \quad (1)$$

$$Co(OH)_2 \longrightarrow CoO + H_2O \quad (2)$$

In this experiment, we have observed that the refluxing time and temperature are very crucial parameters for the formation of CoO-TNs because at optimum refluxing time and temperature, nanostructures are stable but as the refluxing time exceeded, molecules merge with each other and form diverse shaped nanostructures.

3-1-3. Antimicrobial activity of CoO-TNs

A concentration dependent growth inhibition of all four tested strains was observed with CoO-TNs. Growth of *P. aeruginosa* a Gram negative bacterium was inhibited by 1, 15, 20, 23, 27 and 34% with 25, 50, 100, 200, 300 and 500 μg/ml of CoO-TNs, respectively (Fig. 5a). While the growth of *E. coli* decreased by 4, 2, 7, 20, 30 and 39% with 25, 50, 100, 200, 300 and 500 μg/mL of CoO-TNs, respectively (Fig. 5b). The growth of Gram positive bacteria *M. luteus* was inhibited by 25, 47, 76, 98, 99 and 98% with 25, 50, 100, 200, 300 and 500 μg/ml of CoO-TNs, respectively (Fig. 6a). And a growth inhibition of 13, 53, 58, 59, 62 and 65% was observed for another Gram positive bacteria *S. aureus* with 25, 50, 100, 200, 300 and 500 μg/mL of CoO-TNs, respectively (Fig. 6b). It is clear from the comparison of Fig. 5 and Fig. 6 that CoO-TNs is more effective against Gram positive bacteria than the Gram negative bacteria tested in this study. In Gram negative bacteria the significant (p <0.05) inhibition of growth was observed only at a concentration of 100 μg/ml or higher (Fig. 5). However, the significant (p <0.05) inhibition of growth of tested Gram positive bacteria was observed even at a concentration of 50 μg/mL or higher. Moreover, it is also evident from the Fig. 5 and 6 that the concentration dependent inhibition of growth was more prominent in Gram positive bacteria than in Gram negative bacteria tested.

Although, currently there is no clear evidence to interpret the species sensitivity in terms of bacterial classification (Gram + and Gram −), but selective antimicrobial activity of NPs such as silver nanoparticles (Ag-NPs) copper oxide nanoparticles (CuO-NPs) and zinc oxide nanoparticles (ZnO-NPs) has been reported earlier also [22-24].

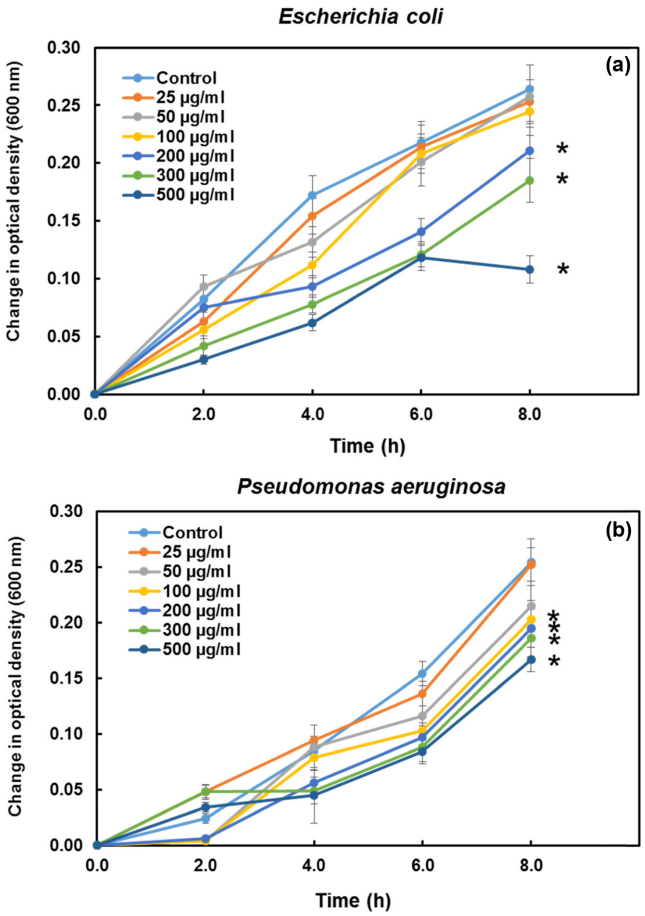

Fig. 5. Growth prevention of Gram negative bacteria (a) *E. coli* and (b) *P. aeruginosa* with various concentrations of CoO-TNs. Error bars show standard deviation and asterisk indicate significant values (p < 0.05).

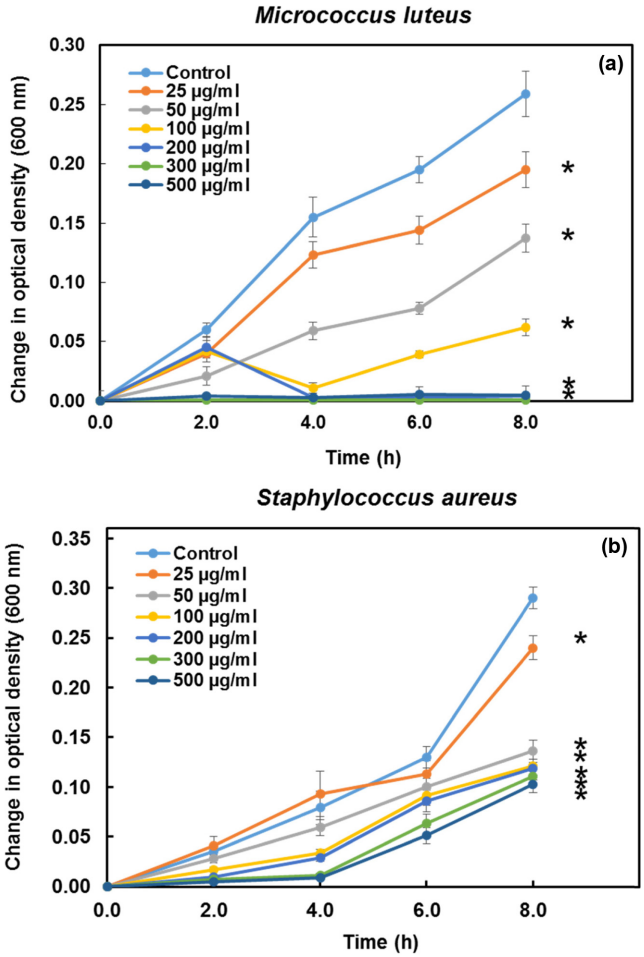

Fig. 6. Growth inhibition of Gram positive bacteria (a) *M. luteus* and (b) *S. aures* of with various concentrations of CoO-TNs as a measure of optical density 600 nm. Asterisk represents significant values (p < 0.05) and error bars indicate standard deviations.

In these studies the tested NPs (Ag-NPs, CuO-NPs and ZnO-NPs) were found to be more effective against the Gram positive bacteria than Gram negative bacteria. In another similar study the antimicrobial activity of CoO-NPs with as average size of 9.13 nm against *Bacillus subtilis* (Gram positive) and *Salmonella typhimurium* (Gram negative) was tested, and interestingly the antimicrobial activity was observed only against *Bacillus subtilis* [20]. This difference in activity may be attributed to the biochemical nature of the target bacterium. One of the important factors is the differential biosorption of metals released from nanostructures/metal oxide NPs by bacteria [25]. It is also known that Gram negative bacteria contain an outer membrane containing lipids that are less impermeable to charged molecules [26]. The reasons for selective activity of CoO-NPs and its mode of action against bacteria is a matter for future studies.

4. Conclusions

Based on the results presented in this manuscript it is concluded that controlling reaction parameter is crucial for the synthesis of pure cobalt oxide thin nanosheets (CoO-TNs) with nearly uniform shape and size, using cobalt nitrate hexahydrate and sodium hydroxide in an aqueous media. Characterization of synthesized nanostructures using XRD and SEM analysis shows that grown structures of CoO exhibit a microflower morphology (2-3 μm), composed of 10-20 nm thick and 60-80 nm long nanosheets. Our study found that the grown CoO-TNs shows excellent antimicrobial activity against Gram positive and Gram negative bacteria and behave as a new antimicrobial agents at 500 μg/mL. The detailed mechanism of the CoO-TNs antimicrobial activity warrants further studies.

Acknowledgments

This project was funded by the National Plan for Science, Technology and Innovation (MAARIFAH), King Abdul Aziz City for Science and Technology, Kingdom of Saudi Arabia Award Number (12-NAN-2490-2).

References

1. O. V. Salata, *J. Nanobiotechnol.,* **2**, 1(2004).
2. N. Sanvicens and M. P. Marco, *Trends Biotechnol.,* **26**, 425(2008).
3. L. Zhang, F. X. Gu, J. M. Chan, A. Z. Wang, R. S. Langer, and O. C. Farokhzad, *Hum Mutat.,* **83**, 761(2008).
4. S. T. Khan, M. Ahamed, J. Musarrat, and A. A. Al-Khedhairy, *Eur. J. Oral Sci*., **123**, 397(2014).
5. H. Kim, K. H. Baik, J. Kim, and S. Jang, *Korean Chem. Eng. Res*., **51**, 292(2013).
6. D. T. Nguyen and K.-S. Kim, *Korean J. Chem. Eng*., **31**, 1289 (2014).
7. A. Akberzadeh, M. Samiei, and S. Davaran, *Nanoscale Res Lett.,* **7**, 144(2012).
8. K. Wang, J. J. Xu, and H. Y. Chen, *Biosens. Bioelectron*., **20**, 1388(2005).
9. Q. M. Kainz, S. Fernandes, C. M. Eichenseer, F, Besostri, H. Körner, R. Müller, and O. Reiser, *Faraday Discuss*., (2014).
10. J. R. Thomas, *J. Appl. Phys*., **37**, 2914(1966).
11. D. P. Dinega, M. G. Bawendi, and Angew, *Chem. Int. Ed.,* **38**, 1788(1999).
12. T. O. Ely, C. Pan, C. Amiens, B. Chaudret, F. Dassenoy, P. Lecante, M. J. Casanove, A. Mosset, M. Respaud, and J. M. Broto, *J. Phys. Chem. B*, **104**, 695(2000).
13. J. Devanneaux and J. Maurin, *J. Catal.*, **69**, 202(1981).
14. Y. Teng, H. Sakurai, A. Ueda, and T. Kobayashi, *Int. J. Hydrogen Energy*, **24**, 355(1999).
15. J. S. Chen, T. Zhu, Q. H. Hu, J. Gao, F. Su, S. Z. Qiao, and X. W. Lou, *ACS Appl. Mater. Interfaces*, **2**, 3628(2010).
16. D. S. Wang, X. L. Ma, Y. G. Wang, L. Wang, Z. Y. Wang, W. Zheng, X. M. He, J. Li, Q. Peng, and Y. Li, *Nano Res*., **3**, 1-7(2010).
17. Y. Zhang, J. Zhu, X. Song, and X. Zhong, *J. Phys. Chem. C*, **112**, 5322(2008).
18. G. P. Glaspell, P. W. Jagodzinski, and A. Manivannan, *J. Phys. Chem. B*, **108**, 9607(2004).
19. J. Cordero, L. Munuera, and M. D. Folgueira, *J. Bone Joint Surg. Br*., **76**, 717(1994).
20. J. W. Costerton, L. Montanaro, and C. R. Arciola, *Int. J. Artif. Organs*, **28**, 1062(2005).
21. G. M. Nazeruddin and Y. I. Shaikh, *RJPBCS*, **5**, 225(2014).
22. A. Azam, A. S. Ahmed, M. Oves, M. S. Khan, and S. S. Habib, *Int. J. Nanomed.*, **7**, 6003(2012).
23. M. Khan, S. T. Khan, M. Khan, S. F. Adil, J. Musarrat, A. A. Al-Khedhairy, A. Al-Warthan, M. R. Siddiqui, and H. Z. Alkhathlan, *Int. J. Nanomed*., **28**, 3551(2014).
24. M. Premanathan, K. Karthikeyan, K. Jeyasubramanian, and G. Manivannan, *Nanomed*., **7**, 184(2011).
25. A. Hassen, N. Saidi, M. Cherif, and A. Boudabous, *Bioresour. Technol*., **65**, 73(1998).
26. H. Nikaido, *Microbiol. Mol. Biol. Rev*., **67**, 593(2003).